# Identification of molecular and functional subtypes using chronic pancreatitis patient-derived organoid models

Victoria Osorio-Vasquez*[1], Jan C. Lumibao*[1,2], Kristina L. Peck[1], Kathryn Lande[1], Jonathan Zhu[1], McKenna Stamp[1], Shira R. Okhovat[1], Hyemin Song[1], Satoshi Ogawa[1],Jasper Hsu[1], Yang Dai[1], Angelica Rock[1], Chelsea Bottomley[1], Ethan Thomas[1], Alexandra Fowler[3],T'Onj McGriff[4], Siri Larsen[5], Muhamad Abdulla[5], Phil Greer[6], Jessica Gibson[6], Michael Downes[1], Ronald Evans[1], Jingjing Zou[7], Andrew M. Lowy[7], David C. Whitcomb[7,8], Rebekah White[2], Melena Bellin[9], Herve Tiriac[2], Dannielle D. Engle[1]

[1]Salk Institute for Biological Studies, La Jolla, California, USA.
[2]Bristol Myers Squibb, San Diego, CA, USA.
[3]University of California Riverside, Keck Graduate Institute, Riverside, CA, USA.
[4]University of Alabama, Birmingham, AL, USA.
[5] Schulze Diabetes Institute, Department of Surgery, University of Minnesota Medical School, Minneapolis, MN, USA.
[6]Ariel Precision Medicine, Pittsburg, PA, USA.
[7]Department of Surgery, Division of Surgical Oncology, Moores Cancer Center, University of California San Diego, San Diego, California, USA.
[8]Univeristy of Pittsburg, Pittsburg, PA, USA.
[9] Departments of Pediatrics and Surgery, Division of Pediatric Endocrinology, University of Minnesota Medical School Minneapolis, MN, USA.

*Authors contributed equally

## Abstract

Background and Aims:

Chronic pancreatitis (CP) affects more than 200,000 Americans and 1 million individuals world wide, but treatment generally focuses on supportive care like pain management. 28-80% of CP cases are idiopathic and 10-15% are hereditary with mutations in PRSS1, SPINK1, CFTR, and other genes. Developing human models of pancreatitis to understand the drivers of the disease and targeting key players in this disease will provide novel therapeutic approaches for these patients who have limited options.

Methods:
Utilizing patient samples from surgical resections or TPIAT procedures we have generated a first-of-its-kind human CP patient derived organoid (PDO) biobank. This biobank is representative of hereditary mutations found across patients, includes idiopathic cases, and histologically recapitulates features of this disease. Genetic concordance was determined between PDO and primary specimens using whole

genome sequencing. RNAseq and cytokine analysis was conducted on PDO to determine inflammatory features of this model. Forskolin induced swelling assays were conducted to determine the function of CFTR in PDO models.

Results:
There is a 98% concordance between PDO and primary tissue specimens showing the recapitulation of patient genotypes in our model. RNA-seq revealed that CP organoids are transcriptionally distinct from normal pancreas organoids and identified three distinct subtypes of CP that are driven by transcriptional features. Utilizing the PDO model, we identified a high prevalence of ductal CFTR dysfunction, which could be restored using a combination of CFTR correctors and potentiators.

Conclusions:
There are three subtypes of CP that require further study to employ targeted therapeutics against these drivers. hCP PDO are a model that can be used to assess CFTR function and correction providing evidence for these drugs to be used in CP patients.

Keywords: chronic pancreatitis, patient derived organoids, CFTR

## Introduction

Pancreatitis, or pancreatic inflammation, is a continuum of diseases that progresses from acute to chronic stages. Acute pancreatitis is responsible for >275,000 hospital admissions a year in the USA[1]. 20% of patients have at least one recurrent episode of acute pancreatitis and 30% of patients progress to chronic pancreatitis[2]. The diagnosis of chronic pancreatitis (CP) is made retrospectively, meaning that we do not have a clear way to predict which patients will have recurrent episodes and progress to CP. More than 200,000 Americans and 1 million individuals global have CP[3]. Pancreatitis risk and etiology is assessed using the Toxic-metabolic, Idiopathic, Genetic, Autoimmune, Recurrent and severe acute pancreatitis and Obstructive (TIGAR-O v2) classification. CP is a disease that arises from a combination of environmental and genetic factors that have many overlapping symptoms that are not exclusive to CP (i.e. atrophy, fibrosis, pancreatic exocrine insufficiency, pancreatic pain, diabetes mellitus)[4]. Treatment of CP focuses on supportive care, such as pain management, fluid resuscitation, and antibiotics. Surgery may be used for removal of gallstones and in rare cases, to remove part of the entire pancreas to alleviate severe pain. Gallstones (40-70%)[5, 6], alcohol (7-32%)[7, 8], tobacco (46- >60%)[8, 9], and genetics (10%)[8] are causes for pancreatitis[3], although 28-80% of CP is idiopathic[10].

Mutations in protease serine 1 (*PRSS1*) (68-80%)[11-14], serine protease inhibitor kazal type 1 (*SPINK1*) (1-8.8%)[10, 13], and cystic fibrosis transmembrane conductance regulator (*CFTR*) (16.5%)[13] are most commonly associated with hereditary CP[15, 16]. *PRSS1* and *SPINK1* mutations lead to the dysregulation of digestive enzymes that lead to pancreatic injury, stress, and an inflammatory response[15-20]. Pancreatitis can be initiated in different cell compartments. Acinar cells are often the attributed source of tissue damage in AP due to their production of digestive enzymes. Ductal cells can also contribute to CP

pathology. *CFTR* is the most important molecule for pancreatic duct function. This anion channel is used by ductal cells to secrete sodium bicarbonate[21]. These secretions stimulate mucin production, flush digestive enzymes into the duodenum, and alkalinize acidic chyme from the stomach to provide an optimal pH for pancreatic digestive enzyme activity[22, 23]. 13-37% of hereditary CP patients harbor CFTR mutations, which are more prevalent in pediatric pancreatitis patients[24-31]. The mutation sites associated with hereditary CP are distinct compared to cystic fibrosis patients[24-31]. Importantly, up to 50% of idiopathic CP patients harbor CFTR alterations when extensive genotyping is performed [22, 24-33]. These data suggest that ductal CFTR dysfunction should be studied as a large portion of patients with pancreatitis may benefit from CFTR modulation.

Utilizing 3D organoid culture technology, we can create organoid models from mouse and human normal pancreata and pancreatic adenocarcinoma (PDA) lesions[34, 35]. PDA patient-derived organoids (PDOs) can be rapidly generated from surgical or biopsy material with high efficiency (75-80%)[34-36], greatly improving upon the 10-40% efficiency of previously used 2D or iPSC models[37]. PDOs are robust, reproducible models that enable facile and thorough molecular characterization[36, 38]. These models can be expanded and viably cryopreserved, making research using PDOs widely accessible. PDA PDOs recapitulate the diverse genetic and transcriptomic subtypes of human PDA, reflect patient treatment response, and inform resistance mechanisms[36, 39-43]. These studies demonstrate the utility of PDOs to rapidly predict treatment response, which is now the subject of many clinical trials[44, 45]. A small cohort of pediatric CP PDOs (n=9) were previously generated to investigate communication between ductal cells and islets. While a major advance, we sought to build a comprehensive CP PDO biobank that encompasses the major etiologies and to systematically benchmark the utility of this system to recapitulate key disease features and predict treatment efficacy. We demonstrate a high success rate for PDO generation (70.5%, n=36) and high degree of concordance between PDO and primary tissue specimens at the DNA, RNA, and protein levels. Using these PDOs, we define three distinct molecular subtypes of CP, which may inform treatment and provide new insights into the biology of this disease. We also show that more than 40% of the PDOs tested are deficient in CFTR function. Treatment with CFTR modulators restored ductal function and reduced inflammatory signaling in the organoids. Altogether, this work provides a highly validated platform for the investigation of the molecular mechanisms driving CP and identification of novel therapeutic strategies.

## Methods

### *Human Specimens*

Normal pancreata were obtained from the Lifesharing organ donation program. Pancreatitis tissues were obtained from the University of Minnesota or University of California San Diego. All tissue donations and experiments were reviewed and approved by the Institutional Review Board of University of California San Diego and University of Minnesota. During pancreatectomy, blood supply is preserved to the pancreas as long as possible to avoid prolonged ischemia. The entire pancreas, spleen, and duodenum are removed and the gastrointestinal and biliary continuity is restored by a Roux-en-Y approach. Islet isolation is performed by infusing the pancreas with collagenase and

neutral protease for enzymatic digestion, followed by mechanical disruption using the semi-automated method of Ricordi. The islets are then transported back to the operating room where they are infused intraportally on the same day as the pancreatectomy procedure.

Residual exocrine pancreas tissue following islet isolation is collected for tissue research. Written and informed consent or parental assent, as age appropriate, was obtained prior to acquisition of tissue from all patients.

Tissue specimens were catalogued, imaged, and processed for histology, organoid generation, flash frozen, and viably cryopreserved.

*Organoids, Cell cultures, and culture conditions*

Human specimen tissue was minced and incubated in digestion media (1 mg/mL Collagenase XI + 100 U/mL hyaluronidase- Stem Cell #07919 in DMEM/F12) at 37°C while rotating, fractions were collected every 20 minutes for up to 1 hour, if media became viscous DNAse I (10 µg/mL) was added. Supernatant was collected after a 20-minute incubation and larger tissue pieces were not collected. Supernatant was centrifuged at 300x RCF at 4°C for 5 minutes, at which point the supernatant containing the digestion media was applied to remaining larger tissue pieces. First cell pellet collected was resuspended in 1 mL of HBSS with 2% FBS and placed on ice while collecting additional fractions of digested tissue. After 3 fractions were collected supernatant fraction was washed with Advanced DMEM with 1% glutamax, 1% penicillin/ streptomycin, and 1% HEPES. If larger tissue pieces remained, they were either viably cryopreserved (CrySOfree- Sigma C9249) or plated in Matrigel in separate wells from supernatant. Cells were plated with Matrigel and grown in human complete feeding medium described below. Both human and mouse organoids were maintained in Corning Matrigel from lots 28323001, 2011001, 0287001, and 1062004 during growth, expansion and experiments. No changes in proliferation were observed across Matrigel lots.

Human pancreas, pancreatitis, and mouse organoids were cultured as previously described[36, 38]. Human complete feeding medium contained Advanced DMEM/F12, HEPES, glutamax, B27 supplement, and penicillin/streptomycin (Thermo Fisher Scientific); N-acetylcysteine, nicotinamide (Sigma-Aldrich); hEGF, FGF-10, gastrin, and A83-01 (R&D); rNoggin and rRSPO1 (Qkine LTD); Wnt3a (ImmunoPrecise Antibodies); PGE2 and Y-27632 dihydrocholoride (Tocris Bioscience) as previously described[36]. This media was used during isolation and maintenance of organoid cultures. Mouse organoid media lacked Wnt3a and PGE2. Organoid nomenclature is defined as: hNP, human normal pancreas; hCP, human chronic pancreatitis, mN, murine normal pancreas. All organoid models were routinely tested for *mycoplasma* at Salk Institute.

*Histology and immunohistochemistry*

Tissues were fixed in 10% neutral buffered formalin for 48 hours. Tissues were embedded in paraffin and stained with hematoxylin and eosin or Masson's trichrome by the Tissue

Technology Shared Resource supported by the National Cancer Institute Cancer Center Support Grant (CCSG Grant P30CA23100). The following primary antibodies were used for immunohistochemical staining: Ki-67 (8D5- CST 9449), Troma-III (CK19) (Developmental studies hybridoma bank), CFTR (M3A7- MA5-11768), Cancer Antigen 19-9 (MBS850562). Secondary antibodies used were ImmPRESS® HRP Horse Anti-Mouse IgG Polymer Detection Kit (MP-7402) or ImmPRESS® HRP Goat Anti-Rat IgG Polymer Detection Kit (MP-7404) with ImmPACT® DAB Substrate Kit (HRP) (SK-4105). Staining intensity was semi quantitatively scored as: low, medium, or high using QuPath 0.5.0[46] and ranking percent positive staining. Slides were imaged using the Olympus VS-120 virtual slide scanning microscope or Olympus BX43 Microscope. Zen blue was used to visualize and annotate images.

*Immunoblot*

Standard techniques were employed for immunoblotting of human organoids. Organoids were isolated from Matrigel using cell recovery solution on ice with 0.5x protease and phosphatase inhibitor (Thermo fischer scientific). Organoids were centrifuged at 0.8 x 1000 RCF at 4°C to pellet organoids and remove cell recovery solution. Cell pellet was resuspended in TNET with protease and phosphatase inhibitors and incubated on ice before clarifying lysates for whole cell lysate isolation. Protein quantification was carried out using BCA assay (Thermo Scientific- 23227). Protein lysates used to probe for CFTR were warmed to 37°C for 1 hour to prevent insolubility. Protein lysates were separated on a 4%-12% Bis-Tris NuPage gel (Invitrogen). Western blots were probed with at a dilution of 1:1000 for CFTR (CST-78335), CA19-9 (MBS850562), pEGFR (CST- 3777), EGFR (CST- 4267), pSTAT3 (CST- D4XC3), STAT3 (CST- 63585), pAKT (CST- 4060), AKT (CST-4685), pERK (CST- 4370S), ERK2 (CST- 4695), CA2 (Abcam- ab124687), SPINK1 (RnD- AF7496), and Cofilin (CST). Secondary antibodies used were Peroxidase AffiniPure™ Goat Anti-Mouse IgG (H+L) (115-035-003), Peroxidase AffiniPure™ Donkey Anti-Rabbit IgG (H+L) (711-035-152), Peroxidase AffiniPure™ Goat Anti-Rabbit IgG (H+L) (111-035-003), and Sheep IgG Horseradish Peroxidase-conjugated Antibody (HAF016). Western blots were developed using either a film processor (Mini-Med 90-AFP Manufacturing Corporation) or Odyssey M (LiCor). Quantification of immunoblots was conducted using either ImageJ or Empiria Studio.

*WGS library preparation, sequencing, variant calling, and primary tissue- organoid SNP concordance*

Genomic DNA was isolated from organoids or primary tissue using DNeasy Blood and Tissue Kit (Qiagen- 69504). WGS libraries were prepared using Nextera XT (Illumina DNA library) in accordance with the manufacturer's instructions. Final libraries were evaluated using TapeStation (Agilent). Libraries were sequenced on an Illumina NovaSeq X sequencer for 30 x coverage for primary tissues and PDO.

Raw data was aligned to the hg38 reference genome with bwa mem v0.7.12-r1039. PCR duplicates were marked with Picard v1.130, and germline variants were called with GATK's haplotypecaller, v4.0.8.1. SNPs and INDELs were filtered with vcftools v0.1.13

the parameters: max-missing=0.5, mac=2, min-meanDP=15, minQ=32. For the purposes of concordance testing, multi-allelic sites and sites with missing genotype calls were discarded.

Concordance was determined using R 'irr' package (version 0.84.1) using intraclass correlation coefficient (ICC) using a two-way model with a 0.95 confidence level.

*RNA isolation and RNA-seq library construction*

For RNA-seq experiment, organoids in Matrigel were lysed directly with 1 mL of TRIzol reagent (Thermo Fischer), and total RNA was extracted using RNeasy Mini Kit (Qiagen). RNA quality control was performed on all samples using Qubit Fluorometer (Invitrogen) and TapeStation (Agilent) before RNA-seq analyses. Library construction was conducted using Novaseq 6000 sp reagent kit v 1.5. Samples were sequenced 300 cycles for 150 bp paired end reads.

*RNA-seq analysis, PCA visualization, and differential gene expression analysis*

Raw reads were quality checked with FASTQC (v0.12.1). Poor quality 3' ends and sequencing adapters were trimmed with Cutadapt (v4.9) and reads shorter than 20nt were filtered. Trimmed reads were again checked with FASTQC, then aligned to human reference genome (hg38 from UCSC with gene annotation gencode.v45.basic.annotation.gtf) and genes quantified with STAR (2.7.11b). Subsequent analysis was performed in R.

The column with 2$^{nd}$ read strand aligned with RNA from the STAR generated expression tables were used since the library prep was strand specific. Expressions were normalized with DESeq2 and the top 500 most variable genes after variance stabilization were used for the PCA plot and heatmap. DESeq2 was also used for differential gene analysis, with cutoffs $padj < 0.05$ and $|log_2 FoldChange| > 1$. These values plotted in the volcano plot for every gene.

Nonnegative matrix factorization exclusively for hCP was performed with the NMF library. Ranks 2 through 7 were tested, each with 500 runs to determine the optimal rank. Based on consensus throughout 500 runs, as well as the rank survey scores from the best run each rank, rank 3 was picked as the optimal rank. The consensus shows the best run from the 500 and which samples clustered together but basis was the parameter used to determine the most stable subtypes.

Differential gene analysis was performed again, this time separated by basis found with NMF.

Heatmaps are generated with pheatmap, all other figures are generated with ggplot2. R version and library versions are below.

*Forskolin induced swelling assay*

Organoids were seeded into 96-well black well clear bottom plates in 8 µL domes at a confluency between 50-70%. Organoids were fed human complete medium after seeding. 18-12 hours prior to treatments, media was changed and $PGE_2$ was removed from media. Organoids treated with inhibitors (CFTRinh-172- Selleck Chemicals S7139; PPQ-102- Selleck Chemicals S1565; H-89- Fisher 501873404) incubated for 2 hours prior additional treatments with forskolin (Selleck- S2449), CFTR potentiators (Icenticaftor (QBW251)- Selleck S9973; Ivacaftor- Medchem express HY-13017; Ivacaftor- Selleck S1144), CFTR corrector (Lumacaftor- Selleck S1565; Elexacaftor- Medchem Express HY 111772, Selleck S8851; Tezacaftor- Selleck S7059). Mouse normal organoids treated with forskolin were used as a positive control for assay. All compounds were dispensed using a Tecan HP D300e. Organoids were imaged using brightfield imaging on Tecan Spark Cyto. Images were taken at time of treatment and 6 hours post treatment. The area of 10 organoids was measured at these two time points using either QuPath 0.5.0 or ImageJ. The relative area at 6 hours was used for comparison across treatment groups. T-tests and ANOVA statistical tests were conducted.

*Data visualization*

Data was visualized using R studio (2024.04.2+764) and Graphpad prism. Figures were arranged in Adobe Illustrator.

*Data Availability*

Raw data for whole genome sequencing and RNA-seq will be publicly available on NCBI Gene Expression Omnibus upon final publication of manuscript.

## Results

*Chronic Pancreatitis Patient Cohort Characteristics*

For generation of the hCP PDO biobank (Table 1, Figure 1A-B), 51 samples were received. Thirty-three patients were female (65%), and the mean age was 38.24 years (range: 11-71). White non-Hispanic patients were the majority of our cohort. CP samples were isolated primarily from total pancreatectomy islet auto transplantation (TPIAT) procedures (75%). Idiopathic CP represented 41% of the CP patients (Figure 1C). The most common mutations were reported for the patients that received genetic testing were in CFTR (31%), PRSS1 (16%), and SPINK1 (13%).

**Table 1.** Characteristics of patients (n=51).

| ***Demographics*** | ***PDO established (n=36)*** | ***PDO not established (n=12)/ in progress (n=3)*** |
|---|---|---|
| Age, y, range (SD) | 11-71(18.9) | 11-71 (17.0)/ 18-60 (21.1) |
| Female sex, n (%) | 24 (66) | 7 (58)/ 2 (66) |
| Male sex, n (%) | 12 (33) | 5 (42)/ 1 (33) |
| Race | | |
| White, n (%) | 28 (77) | 7 (58) / 1 (33) |
| Hispanic, n (%) | 4 (11) | 1 (8.3) / 2 (66) |
| Black, n (%) | 1 ( 2.7) | 1 (8.3) |
| Multi-racial, n (%) | 1 (2.7) | 2 (16.6) |
| Not reported | 2 (5.5) | 0 (0) |
| ***Procedure*** | | |
| Partial Pancreatectomy (total =16), n (%) | 7 (19) | 7 (19)/ 0 (0) |
| TPIAT (total = 35), n (%) | 27 (75) | 8 (66)/ 3 (100) |
| ***Etiology*** | | |
| Genetic | 16 (44) | 2 (16.6)/ 0(0) |
| Idiopathic | 12 (33) | 8 (66)/ 1(33) |
| Alcohol | 3 (25) | 0(0)/ 0(0) |
| Obstruction | 1 (2.7) | 0(0)/ 0(0) |
| Solid-pseudopapillary neoplasm | 1 (2.7) | 0(0)/ 0(0) |
| Divisium + Genetic | 2 (5.5) | 2 (16.6) / 1(33) |
| Groove | 1 (2.7) | 0(0)/ 0(0) |
| Sphincter of oddi dysfunction | 0 (0) | 0(0)/1(33) |
| ***Mutations*** | | |
| PRSS1 | 6 (16.6) | 2 (16)/ 0(0) |
| SPINK1 | 7 (19) | 0 (0)/ 0(0) |
| CFTR | 14 (39) | 2 (16)/ 0(0) |

*Chronic Pancreatitis Patient-Derived Organoid Generation*

PDOs were established from specimens of CP patients who underwent either partial pancreatectomy or TPIAT procedures. Pancreatectomy specimens varied in size and showed signs of cautery. TPIAT specimens were received partially dissociated. Fat, mesentery, and calcifications were removed from specimens prior to processing for PDO

generation. When sufficient intact material was available, a portion of the specimens were fixed upon arrival for histology. Samples from pancreatectomy had intact parenchyma (hCP3), but samples from TPIAT procedure had disrupted parenchyma due to their partial dissociation prior to receipt (hCP11 and hCP17) (Figure 1A). Samples from CP patients recapitulate the triad of histopathological features of CP: fibrosis, atrophy, and ductal changes (Figure 1A, MT and H&E). Fibrosis scoring was reported for TPIAT patients and matched our histological analysis of samples (Figure 1B). Patient history detailed mutations found through genetic testing or known family history (Figure 1C). *PRSS1* mutations are the most common mutation in hereditary chronic pancreatitis[3, 15], with R122H being the most common alteration followed by N29I and A16V[15]. R122H, N29I, and A16V represent three activating mutations that are pathogenic and lead to autocatalytic activation of the enzyme. Although not considered pathogenic, the E79K mutation activates PRSS2 leading to similar prolonged activation of trypsinogen in the pancreas[47]. R116C is a rare mutation that induces misfolding and intracellular retention of PRSS1 leading to ER stress, which is likely pathogenic[48]. These *PRSS1* variants were present in 16% of the CP patients from which PDOs were generated, reflecting their penetrance in the disease (Figure 1C). *SPINK1* mutations are found in 1-8.8%[8] of hereditary CP cases and 50% of idiopathic CP cases[10]. 19% of the CP patients were *SPINK1* mutant, harboring the prevalent N34S mutation[49] (Figure 1C). The effects of *SPINK*$^{N34S}$ mutation remain elusive but do not alter secretion or trypsin inhibitory activity; however this mutation is associated with acute pancreatitis[50]. In 31% of the patient cohort, *CFTR* had disease associated mutations at Q1352 and E217G, along with other common mutations and poly T variants (5T/7T/9T)[51]. The patient characteristics reflect common disease associated mutations in CP.

Patient specimens were minced and aliquoted for viable cryopreservation for potential regeneration of PDOs, flash frozen for primary tissue DNA extraction, and the remaining sample was digested for PDO generation. We successfully generated organoids from 71% of CP specimens (Figure 1D). Failures occurred when tissue was frozen upon arrival (n=2), leading to no viable tissue, or a lack of epithelial cells in the specimen due to extensively fibrosis. We had a higher degree of success generating CP PDOs from TPIAT relative to partial pancreatectomy samples, 77% and 56%, respectively (Figure 1D). After 3-7 days in culture, organoid growth was observed from either tissue digestion supernatant or minced tissue embedded in Matrigel. CP organoids have clear cystic lumen with a thin epithelial layer. The CP PDOs can be passaged 12-20 times before organoids decrease proliferation (Figure 1E), which is in line with what is observed in normal pancreas organoids. Regardless of CP etiology, organoids have similar morphologies.

*Genetic, Histologic, and Protein Expression Concordance*

We conducted genomic, histologic, and immunoblot analyses to assess how well PDOs replicate the characteristics of CP. DNA and whole cell lysates were isolated after a minimum of 3 passages from PDOs. Isolation of primary tissue DNA was conducted from either flash frozen or viably cryopreserved samples. Genomic alterations were compared between PDOs and primary tissue by whole genome sequencing (WGS) or targeted sequencing. By WGS, we found a 98% concordance rate with an intra correlation

coefficient of 0.96 between 5 pairs of PDOs and primary tissue (Figure 2A). A more in-depth analysis of CFTR variants for these 5 paired samples revealed that variants are retained in PDOs (Figure 2B). Intronic variants of CFTR are common[29] and were verified in hCP25 and hCP30 (Figure 2B). We assessed coding sequence variants of CFTR in the sample pairs and confirmed the reported patient mutations (Figure 2C). Additionally, we incidentally discovered mutations that had not been previously annotated (i.e. hCP30 CFTR V470M mutation). Studies have reported the CFTR V470M mutation in CP, but initially did not identify a direct disease association[51]. Patients with this mutation do not show clinically altered chloride sweat levels, which are used to assess CFTR function in the clinic[52]. However, two more recent publications report an association with CP and defective CFTR function in the presence of this mutation[53, 54]. Conducting either WGS, whole exome sequencing, or targeted sequencing of CP pathogenic alterations in PDOs and primary tissue confirmed mutations from patient medical history and uncovered previously unannotated mutations (Figure 2D). PDOs provide the opportunity to study the function of these variants.

Immunohistochemistry (IHC) and immunoblotting were used to evaluate how accurately PDOs replicate the expression of markers associated with pancreatitis, as well as mitogenic and inflammatory signaling. By immunoblot, CP and normal pancreas (NP) PDOs exhibited protein alterations consistent with matched patient specimens (Figure 2E). We previously found that up to ~90% of adult CP has local elevation of CA19-9[55]. A subset of our CP PDOs (66%) exhibited elevated levels of CA19-9 (Figure 2E, 2G), which matched patient specimens by IHC (Figure 2F, hCP08). hCP26 and hCP35 patient specimens were CA19-9 negative, which matched in PDOs (Figure 2E-2G). Phosphorylation of STAT3 (Y705) was elevated in a subset of CP PDOs (Figure 2E, 2I), which was also hyperactivated in human CP by IHC (Figure 2E, 2I). Activation of EGFR has been reported in human CP[56]. A subset of hCP PDOs have elevated levels of phospho-EGFR, AKT, and ERK relative to NP PDOs (Figure 2E), suggesting there are “mitogenic” and “non-mitogenic” CP subtypes. NP PDOs exhibits primarily mature CFTR by immunoblot (C band, 150-160KD[57]) with very little immature CFTR (B band, 135-140KD[57]) (Figure 2E). Of those with *CFTR* mutations hCP11 and hCP44 had low levels of mature CFTR (Figure 2E). This corresponds with what is known of about the premature stop codon mutation present in hCP11 and compound *CFTR*$^{R347P;\ R117H}$ mutation that has been reported to lead to major folding defects, and as expected does not produce mature CFTR[58]. E217G and R75Q *CFTR* mutations found in hCP8 and hCP17, respectively, impact anion channel function[51, 57], but not protein maturation. These two lines have mature CFTR, as predicted. Unexpectedly, mature CFTR is absent from non-hereditary, idiopathic hCP26. In hCP15, a non-hereditary case attributed to alcohol and hypothyroidism, also demonstrated loss of mature CFTR protein despite being CFTR wild type by targeted sequencing (data not shown). Decreased CFTR expression and function as a result of alcohol[21, 59], tobacco[60], and hypothyroidism[61] has been shown. These findings suggest that CFTR potentiators, which raise the basal activity of CFTR, may help even *CFTR* wildtype CP patients. CFTR expression in PDOs generally matches patient specimens (Figure 2E-2F). These findings show that both hereditary and non-genetic factors can affect CFTR in CP PDOs. Carbonic anhydrase 2 (CA2), which catalyzes the conversion of $CO_2$ into $HCO_3^-$, was decreased in most CP PDOs when compared to hNP, pointing to another possible mechanism through which $HCO_3^-$ transport may be impaired

in CP (Figure 2E). SPINK1, which regulates trypsin activation and is most prominently expressed by acinar cells, was decreased in 2 CP PDOs (Figure 2E). Together, these data support that PDOs retain key molecular and genetic features of CP.

*Transcriptomic profiling of normal, normal adjacent to tumor, and pancreatitis PDO cultures*

RNA sequencing (RNA-seq) was performed on 24 CP PDOs, 9 NP (head, body, and tail of pancreas), and 4 normal adjacent to tumor (NAT) PDOs. The NP and NAT organoids clustered separately from the majority of CP PDOs by principal component analysis, except hCP11, 15 and 48 (Figure 3A). CP PDOs have a different transcriptomic profile as compared to NP and NAT PDOs (Figure 3B). Differential gene expression analysis comparing CP to NP and NAT PDOs showed an enrichment in metabolic genes related to ion transport and inflammatory responses due to oxidative stress and depletion in genes related to inflammatory signaling (Figure 3C). CP patients often have elevated serum levels of inflammatory cytokines[62]. Compared to NP PDOs, CP had higher levels of fibrosis markers (e.g., *COL1A1*, *TGFB2*) and inflammatory cytokines (e.g., *IL1A*, *CSF1*) (Figure 3D), suggesting that CP PDOs accurately reflect the increased levels of inflammatory cytokines seen in patients.

Ductal lineage identity is maintained by pancreatic PDOs in culture. But, PDOs can arise from acinar cells that undergo metaplasia into ductal cells[63] or non-metaplastic ducts[35, 64, 65]. Acinar cells have historically been the focus of pancreatitis studies, but it has become clear that both acinar and ductal cells contribute to CP[66-68]. Human and animal models (e.g., pig) with *CFTR* mutations cause pancreatic secretions to become more acidic, concentrated, and dehydrated[69, 70]. The premature activation of acinar-derived digestive enzymes and increased proinflammatory and fibrotic signaling pathways is caused by these mutations[71]. Hereditary CP associated with CFTR mutations highlight that CP is a ductal disease as it is exclusively expressed in ductal cells. Xu, Y. et. al. published gene expression data from sorted human acinar and ductal cells and acinar-derived PDOs[63]. Utilizing the transcriptional signatures established in this work we assessed cell lineage genes and markers of acinar or ductal cell of origin (Figure 3E). NP PDOs gene expression matches an acinar cell of origin signature (Figure 3E). The 3 CP PDOs that did not cluster closely with hCP by principal component analysis (Figure 3A) likely arose from acinar cells similar to what was observed in the NP PDOs. These 3 CP organoids may represent non-diseased pancreas. Other CP PDOs had a hybrid phenotype that suggests both acinar and ductal lineages can contribute PDO generation (hCP18, 25, 27). But most CP PDOs exhibit gene expression signatures that suggest a ductal cell origin (Figure 3E).

To further identify how well CP PDOs recapitulate the production of inflammatory cytokines in CP, we evaluated secreted proteins (Eve Tech.). The conditioned medium of 14 CP and 9 NP PDOs was collected. IL1A, TGFB2, CX3CL1, and other fibroinflammatory secreted factors were elevated in hCP PDOs and reflected the changes observed in gene expression and published changes in CP patients[72, 73] (Figure 3F), demonstrating the ability of CP PDOs to model inflammatory changes in patients.

*Subtyping of Chronic Pancreatitis cultures*

Principal component analysis of RNA-seq was conducted on CP PDOs to determine if transcriptional ductal epithelial subtypes exist. CP PDOs formed three clusters with a variance of 34% (Figure 4A). The PDO transcriptomes were also independently clustered using nonnegative matrix factorization (NMF), revealing 3 stable subtypes in hCP PDO cultures (Figure 4B). The molecular subtypes identified using this approach do not cluster according to etiology (Figure 4B), suggesting that this clustering may reveal distinct subtypes independent of TIGAR-O classification. The genes exhibiting differential expression across the 3 subtypes of CP with the highest K-score drive these distinct clusters (Figure 4C). We performed GSEA on the genes differentially expressed between the subtypes. Subtype 3 does not have a positively enriched gene set and instead, is depleted in the gene sets enriched in subtypes 1 and 2. This cluster contains the fewest number of CP PDOs (n=5). Incorporation of additional CP PDOs may be required to sufficiently power these analyses to identify pathways that drive this subtype. Subtype 2 is enriched in Epithelial to Mesenchymal Transition (EMT) and IL6/JAK/STAT3 signaling gene sets. Subtype 1 is enriched in cholesterol homeostasis and mTORC1 signaling. The PDOs with the highest levels of mitogenic signaling by IB (e.g., hCP01, 8, 16, 17, and 44) were also in the first molecular subtype that was enriched in mTORC1 gene set, which is likely driven by the heightened mitogenic signaling in these CP PDOs. The reciprocal enrichment vs depletion of these gene sets across the subtypes reveal the distinct signaling pathways engaged between clusters.

*CFTR modulation in hCP PDOs corrects forskolin induced swelling and increases CFTR expression*

The Forskolin-induced swelling (FIS) assay was first developed to measure CFTR dysfunction in intestinal and rectal organoids and to predict response to CFTR modulators[74, 75]. Intestinal current measurements and FIS activity are tightly correlated meaning it can serve a surrogate for more difficult electrophysiological measurements[75]. First, we optimized the FIS assay in murine normal (mN) pancreatic organoids and hNP PDOs. DMSO control treated organoids had no response, but the forskolin treated organoids swelled (Figure 5A). Swelling was inhibited when mN and hNP organoids were treated with CFTR inhibitors (CFTRi-172, PPQ-102) or a PKA inhibitor (H-89) demonstrating that swelling is dependent on forskolin induced activation of CFTR via PKA (Figure 5A). mN organoids served as our positive control for this assay while testing the CFTR function of CP PDOs. CP PDOs with wild type *CFTR* (hCP1, hCP3, hCP26, hCP48) or *CFTR* variants without disease association (hCP49 CFTR Q1352H) swelled in response to forskolin treatment. Although hCP49 is *CFTR* mutant, the Q1352H variant alone has not been shown to alter CFTR function, which is in alignment with our findings[51]. More than 40% of the CP PDOs evaluated (n=4 out of 9) were FIS deficient (Figure 5B). hCP16 has a heterozygous V470M mutation[53, 54] and is FIS deficient (Figure 5B). hCP11 did not swell, which can be attributed to the lack of mature CFTR due to the premature stop codon mutation (Figure 2D)[76]. Of note, hCP35 was generated from a presumed non-genetic adult CP patient with mature CFTR levels within normal ranges (Figure 2E), but was found to have a V470M alteration upon WGS in addition to the reported PRSS1

mutation (Figure 2D). This PDO was also FIS deficient (Figure 5B). hCP44 was FIS deficient, which was expected as the patient has multiple CFTR mutations that have been shown to impact FIS (R347P , R117H, V470M, and 7T)[77] and little mature CFTR protein (Figure 2E). We hypothesized that organoids deficient in FIS could be rescued by FDA approved CFTR potentiators for *CFTR* mutants that have altered channel activity. As expected, hCP11 did not swell even after treatment with potentiators, as the mutation does not impact channel activity but rather mature CFTR expression (Figure 5C). hCP35 is FIS deficient and can be corrected by treatment with CFTR potentiators, Ivacaftor and Incenticaftor (Figure 5D). Another approach to increase functional CFTR is treatment with correctors, this class of drugs increases the correct folding and plasma membrane localization of CFTR and the combination of correctors and potentiators has been FDA approved (e.g., Orkambi: Ivacaftor, Lumacaftor)[78]. hCP44 FIS could be rescued by treatment with a combination of correctors and potentiators (Orakambi, and Ivacaftor + Elexacaftor) (Figure 5E, 5F). This demonstrates that our PDO model can used to test CFTR function in variants with known and unknown disease association through FIS and generate treatment paradigms that can improve CFTR function.

How some of the CFTR corrector and potentiator combinations improve CFTR function is not clearly understood in CP. It has been shown in intestinal organoids with CFTR F508del that treatment with elexacaftor, tezacaftor, and ivacaftor (ETI) can restore CFTR function through increased CFTR expression[79]. We tested if treatment with CFTR correctors and potentiators could increase mature CFTR in hCP35 (*CFTR*$^{V470M}$) and hCP44 (*CFTR*$^{R347P,R117H,V470M,7T}$). Single agent Ivacaftor treatment marginally increased mature CFTR in hCP35, but decreased mature CFTR in hCP44 (Figure 5G, 5I). It has been previously shown that Ivacaftor treatment can interfere with mature CFTR stability in the background of certain mutations, requiring more careful and longitudinal study for combination treatments[80]. Treatment with ETI in hCP35 and hCP44 increased mature CFTR expression (Figure 5G-J). This provides evidence that patients with *CFTR*$^{V470M}$ alterations could benefit from ETI treatment to increase mature CFTR expression. CP patients with compound CFTR alterations like those found in hCP44 could also benefit from ETI treatment. Treatment with ETI also led to a decrease in pERK and pSTAT3 levels (Figure 5I, 5J). These data suggest that restoration of CFTR function can decrease fibroinflammatory signaling in CP PDOs. We demonstrate that CP PDO models can be used to study CFTR function and provide new insights into treatments efficacy in the setting of complex mutational landscapes.

## Discussion

The use of PDOs as surrogates to study subtypes of pancreas cancer and functional precision medicine has been established[36, 38, 40, 81]. Here we have generated a groundbreaking CP PDO biobank with the aim to study the molecular and functional subtypes of CP. Primary tissue and matched CP PDOs have a high concordance and are representative of the mutational landscape[18, 20, 49, 51] and inflammatory signatures of CP [15, 82], as previously reported. A limitation of this study is the racial composition of our patient cohort. Although it is well-documented that Black individuals are two to three times more likely to be diagnosed with CP than White individuals[83], our cohort primarily consists of White patients. In addition, CP predominantly affects males; however, our cohort is

primarily female. This may be due to a higher prevalence of hereditary CP[84], higher resection and intervention rate in female patients[85], and female CP cases are increasing. These epidemiological discordances may also be due to social, economic, and access to care factors. Additional studies in these groups are necessary to explore potential biological implications of these factors. Our CP PDO models include relevant mutations in CP and enable the testing of treatments. Other genetic animal models of CP are able to model aspects of pancreatic atrophy, fibrosis, but most lack ductal dysfunction[86, 87] or do not reliably generate CP[88]. CP PDOs exhibit increased secretion of cytokines associated with CP and as a result the alteration of inflammatory signals can be studied in this model.

The subtypes we defined in this work are not completely driven by etiologies, suggesting that underlying cell signaling pathways contribute to CP types. Gene set enrichment analyses revealed distinct pathways in each subtype. Subtype 3 had the least number of differentially expressed genes likely due to the limited number hCP PDOs in this subtype. Subtype 2 was enriched in EMT, which supports a link between chronic inflammation and tumorigenesis. EMT markers have been shown to be elevated in CP and PDA through TGFβ[89], which was elevated in PDOs in this subtype. Elevations in IL2 and STAT5 signaling are also seen in subtype 2, suggesting that this subtype is driven by inflammatory signaling. Subtype 1 has the largest number of PDOs. Genes that significantly drive this subtype are metabolic in nature (i.e. GPX3 and AQP1). The link between inflammation and unresolved reactive oxygen species leading to tissue injury has been established[90]. AQP1 suggests that the ductal function of this subtype is particularly impaired as this traditional water channel has been shown to transport bicarbonate as well[91]. p53 activation has been shown to limit metaplastic transformation in murine pancreatitis models[92]. p53 activation in this basis is coupled with reduced PI3K-AKT-mTOR signaling, indicating that this subtype may be actively counteracting malignant transformation. These subtypes offer a framework to explore and modulate signaling pathways for enhancing ductal and pancreatic function in CP.

An emerging aspect of inflammation in the pancreas is how episodes of inflammation cause epigenetic alterations. Just one bout acute pancreatitis causes lasting effects in the epigenetic landscape[93], which may contribute to disease progression or susceptibility to future pancreatic dysfunction. In the future, studying the epigenetic variations between the subtypes identified in this work may provide valuable insights into pathways that could be targeted to promote pancreatic health.

CP PDOs allow us to study the impact of variants and subtypes on CFTR function. $CFTR^{V470M}$ has been previously reported in patients but is not associated with Cystic Fibrosis, but has been found to associate with chronic pancreatitis[53, 54]. Current genetic sequencing panels may not screen for V470M given its conflicting pathogenicity. Our study shows that in isolation (hCP16) or in complex mutational context (hCP35 and hCP44) $CFTR^{V470M}$ PDOs are deficient in FIS (Figure 5D-E), although there are also other exogenous sources of CFTR dysfunction, such as alcohol and tobacco use. The impaired swelling in these PDOs can be corrected with dual CFTR potentiator and corrector treatment. Reduction in STAT3 signaling following ETI treatment suggests that improving CFTR function decreases inflammatory signaling. This provides a rationale for how improving ductal function can target inflammation in CP. CFTR mutations are present in CP[29, 31] and our data suggest that a large number of CP patients may benefit from CFTR

modulators. Despite their potential, CFTR modulators are not FDA-approved for treating CFTR-related pancreatitis, and health insurance does not cover them, leaving patients with prohibitively high costs[60]. Our CP PDOs provide a platform to assess ductal function and treatment response in CP patients. A limitation of this current work is the sample source. Most CP patients will not undergo surgery. Of note, we demonstrate that PDOs can be generated from pancreatic juice (n=2), which is more routinely obtained as part of CP patient care. Future work will be needed to evaluate the suitability of these pancreatic secretions for representing key CP disease features. Overall, determining the molecular pathways through which ductal malfunction results in CP will facilitate the implementation of focused treatments that optimize health and restore function.

**Conclusion**

In summary, this study demonstrates the potential of CP PDOs as a versatile model for exploring the molecular and functional heterogeneity of chronic pancreatitis. By establishing a biobank of PDOs that closely mirror primary tissues in terms of mutational and inflammatory landscapes, we can gain new insights into the pathogenesis of CP and identify critical pathways for targeted therapeutic interventions. Our findings highlight specific molecular subtypes with distinct signaling profiles. The ability of CP PDOs to replicate key disease characteristics and capture the impact of CFTR mutations illustrates their value in refining precision medicine strategies. This platform not only allows for the rapid assessment of ductal function but also opens avenues for testing novel therapeutic combinations. Future research should aim to refine these models to investigate racial and gender disparities in CP incidence, alongside epigenetic alterations to understand the role of these factors in CP progression. This approach could ultimately lead to the development of innovative therapies that improve patient outcomes

**Acknowledgements**

The authors would like to extend our deepest gratitude to all the patients who generously consented to participate in this study. The authors would like to thank all the members of the Engle laboratory, the UCSD Biorepository and Department of Surgery, the University of Minnesota Departments of Surgery and Pediatrics, April Williams, Ling Ouyang, and Tzu-when Wang at the NGS Core Facility of the Salk Institute, Elsa Molina at the Single-Cell and Spatial Omics core of the Salk Institute, and Daniela Boassa, Sammy Weiser Novak and Elsie Quansah at the Biophotonics Core Facility of the Salk Institute.

**Funding Statement**

V.O.V is supported through the Salk Institute Cancer Training Grant (2T32CA009370-35A1). J.C.L. was supported through the Salk Institute Cancer Training Grant (T32CA0093790). J.H. was supported through the UCSD Pathways in Biological Sciences T32 Training Grant. This work was supported by the The Razavi Newman Integrative Genomics and Bioinformatics Core Facility of the Salk Institute with funding from NIH-NCI CCSG: P30 CA01495, NIH-NIA San Diego Nathan Shock Center P30 AG068635, and the Helmsley Trust. This work was supported by the Waitt Advanced Biophotonics Core Facility of the Salk Institute with funding from NIH-NCI CCSG: P30 CA01495, NIH-NIA San Diego Nathan Shock Center P30 AG068635, and the Waitt Foundation. This work was supported by the NGS Core Facility of the Salk Institute with

funding from NIH-NCI CCSG: P30 CA01495, NIH-NIA San Diego Nathan Shock Center P30 AG068635, the Chapman Foundation and the Helmsley Charitable Trust. Tissue Technology Shared Resource is supported by a National Cancer Institute Cancer Center Support Grant (CCSG P30CA23100). This research program was supported by Mission Cure Capital, LLC, the Lustgarten Foundation, the Conrad Prebys Foundation, The Paul M. Angell Family Foundation, Curebound (20DG11), and by the Helen McLoraine Developmental Chair.

## References


1. E FC, Swaroop VS, Mel WC. Acute Pancreatitis. New England Journal of Medicine 2016;375:1972-1981.
2. Weiss FU, Laemmerhirt F, Lerch MM. Etiology and Risk Factors of Acute and Chronic Pancreatitis. Visceral Medicine 2019;35:73-81.
3. Kleeff J, Whitcomb DC, Shimosegawa T, et al. Chronic pancreatitis. Nature Reviews Disease Primers 2017;3:17060.
4. Whitcomb DC, Group NAPS. Pancreatitis: TIGAR-O Version 2 Risk/Etiology Checklist With Topic Reviews, Updates, and Use Primers. Clinical and Translational Gastroenterology 2019;10:e00027.
5. Tenner S, Baillie J, DeWitt J, et al. American College of Gastroenterology Guideline: Management of Acute Pancreatitis. Official journal of the American College of Gastroenterology | ACG September 2013;108.
6. Crockett SD, Wani S, Gardner TB, et al. American Gastroenterological Association Institute Guideline on Initial Management of Acute Pancreatitis. Gastroenterology 2018/03/01;154.
7. Yadav D, Whitcomb DC, Yadav D, et al. The role of alcohol and smoking in pancreatitis. Nature Reviews Gastroenterology & Hepatology 2010 7:3 2010-02-02;7.
8. Vege SS, Chari ST. Chronic Pancreatitis. New England Journal of Medicine 2022;386:869-878.
9. JS T, L K, U B, et al. Smoking and risk of acute and chronic pancreatitis among women and men: a population-based cohort study - PubMed. Archives of internal medicine 03/23/2009;169.
10. Singh VK, Yadav D, Garg PK. Diagnosis and Management of Chronic Pancreatitis. JAMA 2019;322:2422-2434.
11. AE P, J L, P G, et al. Known genetic susceptibility factors for chronic pancreatitis in patients of European ancestry are rare in patients of African ancestry - PubMed. Pancreatology : official journal of the International Association of Pancreatology (IAP) ... [et al.] 2018 Jul;18.
12. Mutations of the cationic trypsinogen gene in patients with chronic pancreatitis. The Lancet 1999;354.
13. Schwarzenberg SJ, Uc A, Zimmerman B, et al. Chronic Pancreatitis. Journal of Pediatric Gastroenterology and Nutrition 2019/04/01;68.
14. LaRusch J, Whitcomb DC. Genetics of pancreatitis. Current opinion in gastroenterology 2011 Sep;27.
15. Howes N, Lerch MM, Greenhalf W, et al. Clinical and genetic characteristics of hereditary pancreatitis in Europe. Clinical Gastroenterology and Hepatology 2004;2:252-261.
16. Whitcomb DC, Gorry MC, Preston RA, et al. Hereditary pancreatitis is caused by a mutation in the cationic trypsinogen gene. Nature Genetics 1996;14:141-145.
17. Schnúr A, Beer S, Witt H, et al. Functional effects of 13 rare PRSS1 variants presumed to cause chronic pancreatitis. Gut 2014;63:337.
18. Whitcomb DC. Genetic Aspects of Pancreatitis. Annual Review of Medicine 2010;61:413-424.

19. J. Threadgold - The N34S mutation of SPINK1 (PSTI) is associated with a familial pattern of idiopathic chronic pancreatitis but does not cause the disease.
20. Grocock CJ, Rebours V, Delhaye MN, et al. The variable phenotype of the p.A16V mutation of cationic trypsinogen (PRSS1) in pancreatitis families. Gut 2010;59:357.
21. Maléth J, Balázs A, Pallagi P, et al. Alcohol Disrupts Levels and Function of the Cystic Fibrosis Transmembrane Conductance Regulator to Promote Development of Pancreatitis. Gastroenterology 2015;148:427-439.e16.
22. Ooi CY, Durie PR. Cystic fibrosis transmembrane conductance regulator (CFTR) gene mutations in pancreatitis. Journal of Cystic Fibrosis 2012;11:355-362.
23. Moniaux N, Andrianifahanana M, Brand RE, et al. Multiple roles of mucins in pancreatic cancer, a lethal and challenging malignancy. British Journal of Cancer 2004;91:1633-1638.
24. Zoller H, Egg M, Graziadei I, et al. CFTR gene mutations in pancreatitis: Frequency and clinical manifestations in an Austrian patient cohort. Wiener klinische Wochenschrift 2007;119:527-533.
25. Witt H. Chronic pancreatitis and cystic fibrosis. Gut 2003;52:ii31.
26. Truninger K, Malik N, Ammann RW, et al. Mutations of the cystic fibrosis gene in patients with chronic pancreatitis. The American journal of gastroenterology 2001;96:2657-61.
27. Kiesewetter S, Macek M, Davis C, et al. A mutation in CFTR produces different phenotypes depending on chromosomal background. Nature Genetics 1993;5:274-278.
28. Noone PG, Zhou Z, Silverman LM, et al. Cystic fibrosis gene mutations and pancreatitis risk: Relation to epithelial ion transport and trypsin inhibitor gene mutations. Gastroenterology 2001;121:1310-1319.
29. Audrézet M-P, Chen J-M, Maréchal CL, et al. Determination of the relative contribution of three genes–the cystic fibrosis transmembrane conductance regulator gene, the cationic trypsinogen gene, and the pancreatic secretory trypsin inhibitor gene–to the etiology of idiopathic chronic pancreatitis. European Journal of Human Genetics 2002;10:100-106.
30. Lukacs GL, Verkman AS. CFTR: folding, misfolding and correcting the ΔF508 conformational defect. Trends in Molecular Medicine 2012;18:81-91.
31. Cohn JA, Friedman KJ, Noone PG, et al. Relation between Mutations of the Cystic Fibrosis Gene and Idiopathic Pancreatitis. The New England Journal of Medicine 1998;339:653-658.
32. Wiseman AJ, Ooi CY. Clinical Pancreatology for Practising Gastroenterologists and Surgeons, 2021.
33. Ooi CY, Dupuis A, Ellis L, et al. Does extensive genotyping and nasal potential difference testing clarify the diagnosis of cystic fibrosis among patients with single-organ manifestations of cystic fibrosis? Thorax 2014;69:254.
34. Tiriac H, Bucobo JC, Tzimas D, et al. Successful creation of pancreatic cancer organoids by means of EUS-guided fine-needle biopsy sampling for personalized cancer treatment. Gastrointestinal Endoscopy 2018;87:1474-1480.
35. Boj Sylvia F, Hwang C-I, Baker Lindsey A, et al. Organoid Models of Human and Mouse Ductal Pancreatic Cancer. Cell 2015;160:324-338.

36. Tiriac H, Belleau P, Engle DD, et al. Organoid profiling identifies common responders to chemotherapy in pancreatic cancer. Cancer Discovery 2018;8:CD-18-0349.
37. Kim J, Hoffman JP, Alpaugh RK, et al. An iPSC Line from Human Pancreatic Ductal Adenocarcinoma Undergoes Early to Invasive Stages of Pancreatic Cancer Progression. Cell Reports 2013;3:2088-2099.
38. Lumibao JC, Okhovat SR, Peck KL, et al. The impact of extracellular matrix on the precision medicine utility of pancreatic cancer patient-derived organoids. JCI Insight 2023;9:e172419.
39. Grossman JE, Muthuswamy L, Huang L, et al. Organoid Sensitivity Correlates with Therapeutic Response in Patients with Pancreatic Cancer. Clinical Cancer Research 2021;28:clincanres.4116.2020.
40. Gulay KCM, Zhang X, Pantazopoulou V, et al. Dual inhibition of KRASG12D and pan-ERBB is synergistic in pancreatic ductal adenocarcinoma. Cancer Research 2023.
41. Ponz-Sarvise M, Corbo V, Tiriac H, et al. Identification of Resistance Pathways Specific to Malignancy Using Organoid Models of Pancreatic Cancer. Clinical Cancer Research 2019;25:6742-6755.
42. Hou S, Tiriac H, Sridharan BP, et al. Advanced Development of Primary Pancreatic Organoid Tumor Models for High-Throughput Phenotypic Drug Screening. SLAS Discovery 2018;23:574-584.
43. Wolff RA, Wang-Gillam A, Alvarez H, et al. Dynamic changes during the treatment of pancreatic cancer. Oncotarget 2018;9:14764-14790.
44. Letai A, Bhola P, Welm AL. Functional precision oncology: Testing tumors with drugs to identify vulnerabilities and novel combinations. Cancer Cell 2022;40:26-35.
45. Boilève A, Cartry J, Goudarzi N, et al. Organoids for Functional Precision Medicine in Advanced Pancreatic Cancer. Gastroenterology 2024;167:961-976.e13.
46. Bankhead P, Loughrey MB, Fernández JA, et al. QuPath: Open source software for digital pathology image analysis. Scientific Reports 2017;7:16878.
47. N T, C LM, Z K, et al. Interaction between trypsinogen isoforms in genetically determined pancreatitis: mutation E79K in cationic trypsin (PRSS1) causes increased transactivation of anionic trypsinogen (PRSS2) - PubMed. Human mutation 2004 Jan;23.
48. Kereszturi É, Szmola R, Kukor Z, et al. Hereditary pancreatitis caused by mutation induced misfolding of human cationic trypsinogen - a novel disease mechanism. Human mutation 2009 Apr;30.
49. Threadgold J, Greenhalf W, Ellis I, et al. The N34S mutation of SPINK1 (PSTI) is associated with a familial pattern of idiopathic chronic pancreatitis but does not cause the disease. Gut 2002;50:675.
50. O'Reilly DA, Witt H, Rahman SH, et al. The SPINK1 N34S variant is associated with acute pancreatitis. European Journal of Gastroenterology & Hepatology August 2008;20.

51. Lee JH, Choi JH, Namkung W, et al. A haplotype-based molecular analysis of CFTR mutations associated with respiratory and pancreatic diseases. Human Molecular Genetics 2003;12:2321-2332.
52. Zielenski J, Patrizio P, Corey M, et al. CFTR gene variant for patients with congenital absence of vas deferens. Am J Hum Genet 1995;57:958-60.
53. Zhou D, Bai R, Wang L. The Cystic Fibrosis Transmembrane Conductance Regulator 470 Met Allele Is Associated with an Increased Risk of Chronic Pancreatitis in Both Asian and Caucasian Populations: A Meta-Analysis. Genetic Testing and Molecular Biomarkers 2020;24:24-32.
54. Iso M, Suzuki M, Yanagi K, et al. The CFTR gene variants in Japanese children with idiopathic pancreatitis. Human Genome Variation 2019;6:17.
55. Engle DD, Tiriac H, Rivera KD, et al. The glycan CA19-9 promotes pancreatitis and pancreatic cancer in mice. Science 2019;364:1156-1162.
56. CM A, BM G, KK T, et al. EGF receptor is required for KRAS-induced pancreatic tumorigenesis - PubMed. Cancer cell 09/11/2012;22.
57. Cheng SH, Gregory RJ, Marshall J, et al. Defective intracellular transport and processing of CFTR is the molecular basis of most cystic fibrosis. Cell 1990/11/16;63.
58. M vW, AM V, HY Y, et al. Folding-function relationship of the most common cystic fibrosis-causing CFTR conductance mutants - PubMed. Life science alliance 01/18/2019;2.
59. Wilson JS, Pirola RC, Apte MV. Epidemiology and Etiology of Alcohol-Induced Pancreatitis. The Pancreas 2018.
60. MY P, ZM S. Current clinical opinion on CFTR dysfunction and patient risk of pancreatitis: diagnostic and therapeutic considerations - PubMed. Expert review of gastroenterology & hepatology 2022 Jun;16.
61. Gullo L, Pezzilli R, Bellanova B, et al. Influence of the thyroid on exocrine pancreatic function. Gastroenterology 1991;100:1392-6.
62. S R, I V, A M, et al. Chronic pancreatitis: Do serum biomarkers provide an association with an inflammageing phenotype? - PubMed. Pancreatology : official journal of the International Association of Pancreatology (IAP) ... [et al.] 2016 Sep-Oct;16.
63. Xu Y, Nipper MH, Dominguez AA, et al. Reconstitution of human PDAC using primary cells reveals oncogenic transcriptomic features at tumor onset. Nature Communications 2024;15:818.
64. Mun KS, Arora K, Huang Y, et al. Patient-derived pancreas-on-a-chip to model cystic fibrosis-related disorders. Nature Communications 2019;10:3124.
65. M H, P B, SF B, et al. Unlimited in vitro expansion of adult bi-potent pancreas progenitors through the Lgr5/R-spondin axis - PubMed. The EMBO journal 10/16/2013;32.
66. P H, S P, V V, et al. The acinar-ductal tango in the pathogenesis of acute pancreatitis - PubMed. Gut 2011 Apr;60.
67. Pallagi P, Balla Z, Singh AK, et al. The Role of Pancreatic Ductal Secretion in Protection Against Acute Pancreatitis in Mice&ast. Critical Care Medicine 2014;42:e177-e188.

68. P H, OH P. The exocrine pancreas: the acinar-ductal tango in physiology and pathophysiology - PubMed. Reviews of physiology, biochemistry and pharmacology 2013;165.
69. Ooi CY, Uc A. CFTR-Associated Pancreatic Disease. 2023:390-395.
70. Ishiguro H, Yamamoto A, Nakakuki M, et al. Physiology and pathophysiology of bicarbonate secretion by pancreatic duct epithelium. Nagoya J Med Sci 2012;74:1-18.
71. M A-E-H, S R, DK M, et al. Pancreatic damage in fetal and newborn cystic fibrosis pigs involves the activation of inflammatory and remodeling pathways - PubMed. The American journal of pathology 2012 Aug;181.
72. Komar HM, Hart PA, Cruz-Monserrate Z, et al. Local and Systemic Expression of Immunomodulatory Factors in Chronic Pancreatitis. Pancreas 2017;46:986-993.
73. Yasuda M, Ito T, Oono T, et al. Fractalkine and TGF-β1 levels reflect the severity of chronic pancreatitis in humans. World Journal of Gastroenterology : WJG 2008 Nov 14;14.
74. van Mourik P, Michel S, Vonk AM, et al. Rationale and design of the HIT-CF organoid study: stratifying cystic fibrosis patients based on intestinal organoid response to different CFTR-modulators. Translational Medicine Communications 2020 5:1 2020-06-03;5.
75. Dekkers JF, Wiegerinck CL, de Jonge HR, et al. A functional CFTR assay using primary cystic fibrosis intestinal organoids. Nature Medicine 2013 19:7 2013-06-02;19.
76. Bedwell DM, Kaenjak A, Benos DJ, et al. Suppression of a CFTR premature stop mutation in a bronchial epithelial cell line. Nature Medicine 1997 3:11 1997/11;3.
77. Mourik PV, Haaren Pv, Kruisselbrink E, et al. R117H-CFTR function and response to VX-770 correlate with mRNA and protein expression in intestinal organoids. Journal of Cystic Fibrosis 2020;19:728-732.
78. J R, C P-S, IAI S, et al. New drugs in cystic fibrosis: what has changed in the last decade? - PubMed. Therapeutic advances in chronic disease 05/21/2022;13.
79. Lefferts JW, Bierlaagh MC, Kroes S, et al. CFTR Function Restoration upon Elexacaftor/Tezacaftor/Ivacaftor Treatment in Patient-Derived Intestinal Organoids with Rare CFTR Genotypes. International Journal of Molecular Sciences 2023;24:14539.
80. DM C, NL Q, ML F, et al. Potentiator ivacaftor abrogates pharmacological correction of ΔF508 CFTR in cystic fibrosis - PubMed. Science translational medicine 07/23/2014;6.
81. Boilève A, Cartry J, Goudarzi N, et al. Organoids for functional precision medicine in advanced pancreatic cancer. Gastroenterology 2024.
82. Lee B, Jones EK, Manohar M, et al. Distinct Serum Immune Profiles Define the Spectrum of Acute and Chronic Pancreatitis From the Multicenter Prospective Evaluation of Chronic Pancreatitis for Epidemiologic and Translational Studies (PROCEED) Study. Gastroenterology 2023;165:173-186.
83. Lowenfels AB, Maisonneuve P, Grover H, et al. Racial Factors and The Risk of Chronic Pancreatitis. Official journal of the American College of Gastroenterology | ACG March 1999;94.

84. McIlwrath SL, Westlund KN. Prevalence of Pancreatitis in Female and Male Pediatric Patients in Eastern Kentucky in the United States. J Fam Med Community Health 2016;3.
85. Howes N, Lerch MM, Greenhalf W, et al. Clinical and genetic characteristics of hereditary pancreatitis in Europe. Clinical Gastroenterology and Hepatology 2004;2:252-261.
86. OA M, M S, SR M, et al. Lysosome associated membrane proteins maintain pancreatic acinar cell homeostasis: LAMP-2 deficient mice develop pancreatitis - PubMed. Cellular and molecular gastroenterology and hepatology 11/01/2015;1.
87. H A, N J, J K, et al. A mouse model of hereditary pancreatitis generated by transgenic expression of R122H trypsinogen - PubMed. Gastroenterology 2006 Dec;131.
88. Klauss S, Schorn S, Teller S, et al. Genetically induced vs. classical animal models of chronic pancreatitis: a critical comparison. The FASEB Journal 2018;32:5778-5792.
89. Zhao G, Deng S-c, Li X, et al. Chronic pancreatitis and pancreatic cancer demonstrate active epithelial-mesenchymal transition, regulated by the feedback loop between miR-217 and SIRT1. Journal of the American College of Surgeons 2014/10/01;219.
90. Mittal M, Siddiqui MR, Tran K, et al. Reactive Oxygen Species in Inflammation and Tissue Injury. Antioxidants & Redox Signaling 2014 Mar 1;20.
91. ME B, H E. Aquaporin-1 and HCO3(-)-Cl- transporter-mediated transport of CO2 across the human erythrocyte membrane - PubMed. The Journal of physiology 07/15/2003;550.
92. Multifaceted role for p53 in pancreatic cancer suppression. Proceedings of the National Academy of Sciences 2023;120.
93. Poggetto ED, Ho IL, Balestrieri C, et al. Epithelial memory of inflammation limits tissue damage while promoting pancreatic tumorigenesis. Science 2021;373:eabj0486.

**Figure 1. Generating organoids from human chronic pancreatitis (CP) samples.** (A) Representative human normal pancreas (hNP) section displays characteristic ductal, acinar, and islet cells. Masson's trichrome (MT) staining highlights low degree of fibrosis in NP sample and varying severity in human chronic pancreatitis (CP) samples in blue. NP sample has high levels of cytokeratin 19 staining (CK19) in ductal epithelial cells, while CP samples have a loss of the ductal cell compartment. Ki-67 expression is low in NP sample and is altered or completely lost in hCP samples. Scale bar 200 µm. (B) Patient sample cohort demographic, etiology, procedure for acquisition, organoid generation, and fibrosis scoring information. (C) Mutational profile of patient samples as annotated through patient medical history. Mutations in cystic fibrosis transmembrane conductance regulator (CFTR), serine protease inhibitor kazal type 1 (SPINK1), and protease serine 1 (PRSS1) mutations are present in our patient samples representing some of the most common alterations in chronic pancreatitis. (D) Generation efficiency of patient derived organoids (PDOs) from partial pancreatectomy or TPIAT procedure. Cumulative generation efficiency of 71%. (E) Representative images of human organoid cultures established from normal (NP) or chronic pancreatitis (CP), passage is indicated on image. Scale bar 500 µm.

**Figure 2. Human CP organoids recapitulate genomic mutations and protein expression in patient samples.** (A) Genetic concordance, intraclass correlation coefficient (ICC), and 95% confidence interval determined from single nucleotide polymorphisms (SNPs) of hPDO and matched primary tissue specimens by whole genome sequencing (WGS). (B) CFTR variants found along gene with exons highlighted in yellow in PDO and matched primary tissue (PT). Genotype matches reference or is annotated as a heterozygous (HET), homozygous (HOMO), or unknown (UKNOWN) alteration as compared to reference. (C) Coding sequence variants of CFTR in PDO and matched primary tissue (PT) samples. Alterations in amino acids are colored by Grantham distance from reference amino acid. (D) CP PDO mutations in PRSS1, SPINK1, and CFTR determined from either whole exome sequencing, targeted genetic sequencing, or WGS. (E) Immunoblot of hPDOs generated from NP and CP samples. (F) Histological features and immunohistochemistry staining for cancer antigen 19-9 (CA19-9), signal transducer and activator of transcription 3 phosphorylation (pSTAT3), mitogen-activated protein kinase 1 phosphorylation (pERK2), and CFTR of CP samples. (G) Comparison of CA19-9 staining in tissue sections or band intensity of hPDO immunoblot in sample panel. (H) Comparison of pERK staining in tissue sections or band intensity of hPDO immunoblot in sample panel. (I) Comparison of pSTAT3 staining in tissue sections or band intensity of hPDO immunoblot in sample panel.

**Figure 3. Gene expression, and cytokine secretion demonstrate unique alterations in a subset of CP organoids.** (A) Principal component analysis (PCA) of transcriptomic data from organoids isolated from NP, normal adjacent to tumor (NAT), and CP samples. (B) Top differentially expressed genes from variance stabilized gene expression in CP versus NP and NAT samples. ($p$ value $<0.05$, $|\log2\text{fold change}| > 1$) (C) Top 10 differentially enriched genes and top 10 differentially depleted genes in hCP versus NP and NAT. (D) Relative normalized transcript expression of select inflammatory, collagens, and TGFβ genes. Sample disease origin and cluster are denoted. (E) Normalized counts

for ductal, acinar, or islet gene markers in NP, NAT, and CP PDOs. Sample disease origin and cluster are denoted. (F) Secreted protein expression of inflammatory cytokines in NP, NAT, and CP PDOs. P-value determined by Mann-Whitney test.

**Figure 4. Transcriptomic analysis reveals subtypes of CP found in patient samples.** (A) Principal component analysis of transcriptomic data from organoids derived from hCP samples. (B) Clustering using non-matrix factorization (NMF) defines three distinct subtypes of hCP PDO cultures; basis 1, 2, and 3. Patient etiology (A- alcoholic, D- divisum + groove, G- genetic, I- idiopathic, O- obstruction), silhouette, and consensus is indicated. (C) Differentially expressed genes (p value <0.05, |log2fold change| > 1) between three subtypes of hCP with k-scores greater than or equal 0.07 for basis 1 and 2, and greater than or equal to 0.06 for basis 3.

**Figure 5. Cystic fibrosis transmembrane conductance regulator (CFTR) expression or dependent swelling of CP organoids is resolved upon addition of CFTR modulators, potentiators, or correctors.** (A) Forskolin induced swelling (FIS) assay of hNP and mouse normal (mN11) organoids treated with forskolin for 6 hours and pre-treated with CFTR inhibitors (CFTRi-172, PPQ-102), or protein kinase A inhibitor (H-89) for 2 hours. Swelling is inhibited with the addition of CFTR and PKA inhibitors. (B) FIS assay of hCP organoids treated with forskolin for 6 hours. (C) hCP11 containing a $CFTR^{W1282*}$ mutation treated with forskolin, CFTR potentiators (Ivacaftor or icenticaftor), or a combination for 6 hours did not swell as expected. (D) FIS is rescued upon 6 hour CFTR potentiator (Ivacaftor and Incenticaftor) and forskolin treatment in hCP35 PDOs. (E) hCP44 organoids did not swell after 6 hours of treatment with DMSO, forskolin, CFTR potentiator (Ivacaftor), or CFTR corrector (Lumacaftor). (F) hCP44 organoids swelled in response to combination CFTR potentiator (Ivacaftor) and CFTR corrector (Lumacaftor or Elexacaftor) treatment after 6 hours. (G) Mature CFTR expression is increased in hCP35 organoids treated with CFTR potentiator (Ivacaftor) or further increased with ETI (CFTR correctors-Elexacaftor and Tezacaftor, CFTR potentiator-Ivacaftor) for 48 hours. pERK2 and pSTAT3 expression decreases upon ETI treatment. Cofilin is used as loading control. (H) Quantification of immunoblot in H relative to DMSO. (I) Mature CFTR expression increases upon ETI CFTR correctors-Elexacaftor and Tezacaftor, CFTR potentiator-Ivacaftor) in hCP44 organoids treated for 48 hours. pERK1/2 and pSTAT3 is signaling is decreased upon ETI treatment. Cofilin is used as loading control. (J) Quantification of immunoblot in I relative to DMSO.

**Figure 1. Generating organoids from human chronic pancreatitis (CP) samples.**

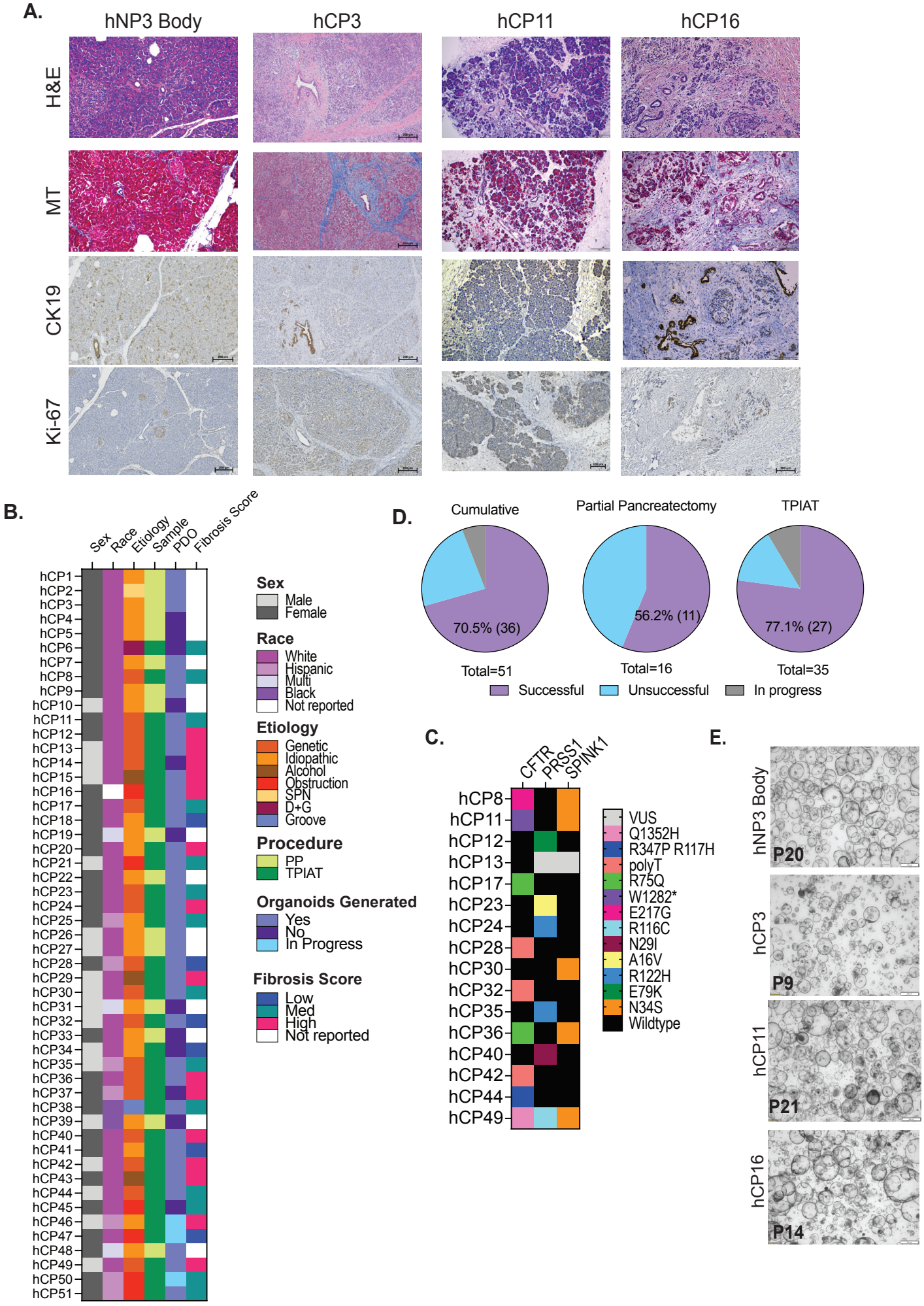

**Figure 2. Human CP organoids recapitulate genomic mutations and protein expression in patient samples.**

**A.**

| | SNPs_Mutant. vs.NonMutant | ICC | 95% Confidence Interval |
|---|---|---|---|
| hCP25 | 98.33% | 0.9665848 | 0.9665491- 0.9666205 |
| hCP28 | 98.26% | 0.9652401 | 0.965203- 0.9652772 |
| hCP30 | 98.30% | 0.9659536 | 0.9659172 -0.9659899 |
| hCP49 | 98.27% | 0.9653908 | 0.9653535- 0.9654281 |
| hCP51 | 98.30% | 0.9659749 | 0.9659384- 0.9660112 |

**B.**

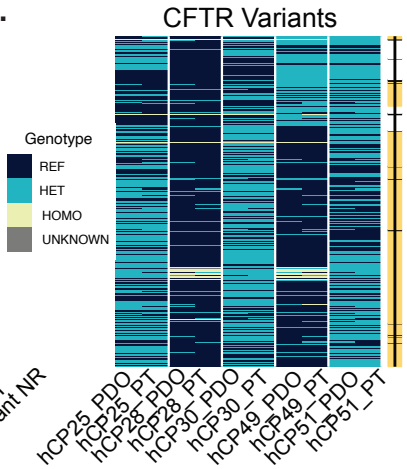


**C.**

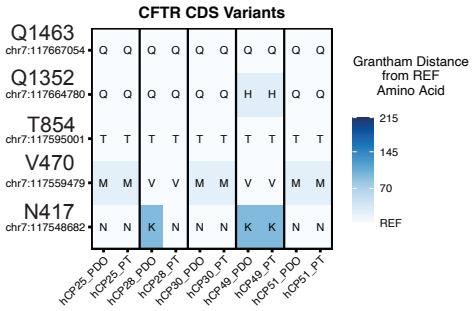


**D.**

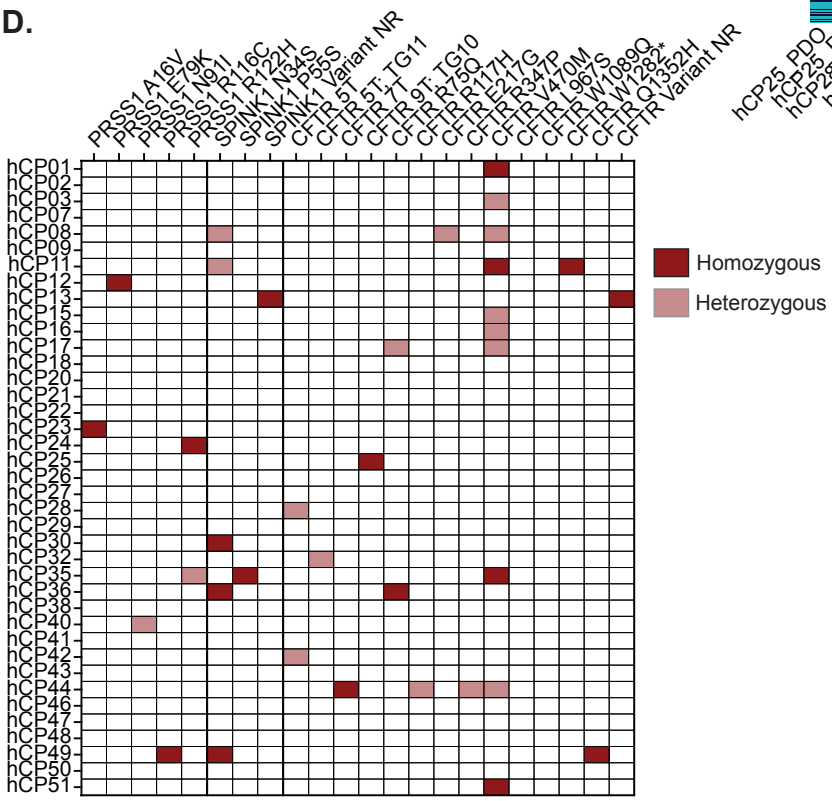


**E.**

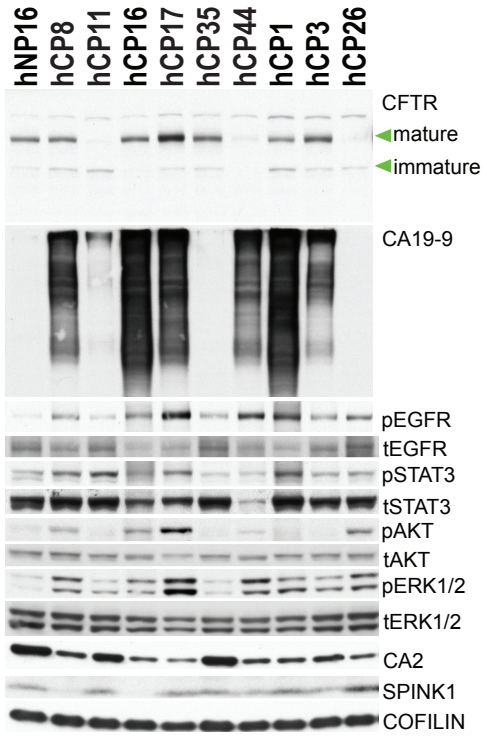


**F.**

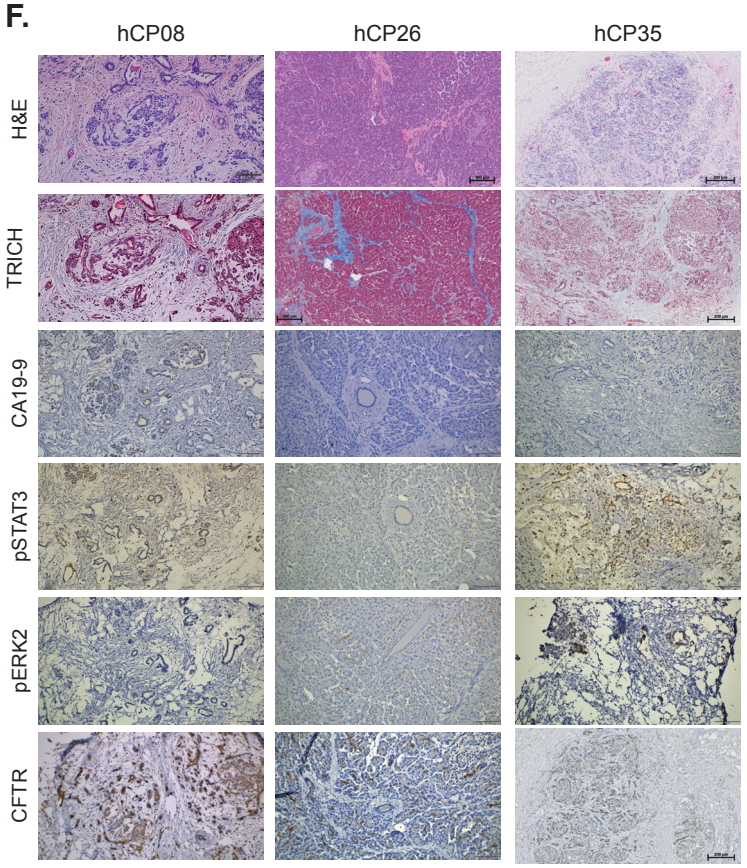


**G.**

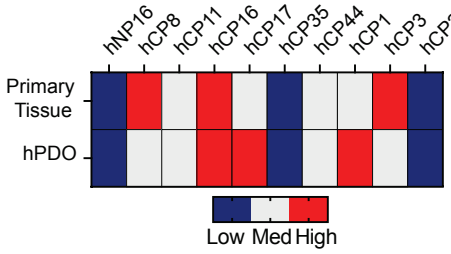


**H.**

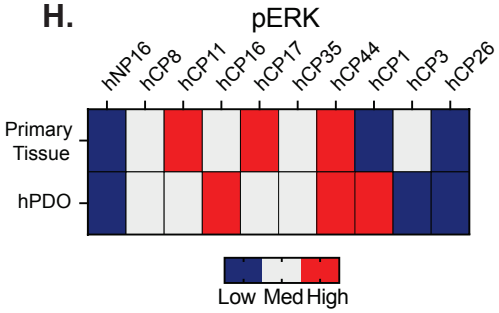


**I.**

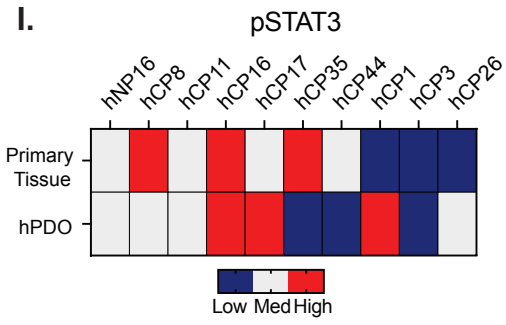

**Figure 3. Gene expression, and cytokine secretion demonstrate unique alterations in a subset of CP patient derived organoids.**

**A.**

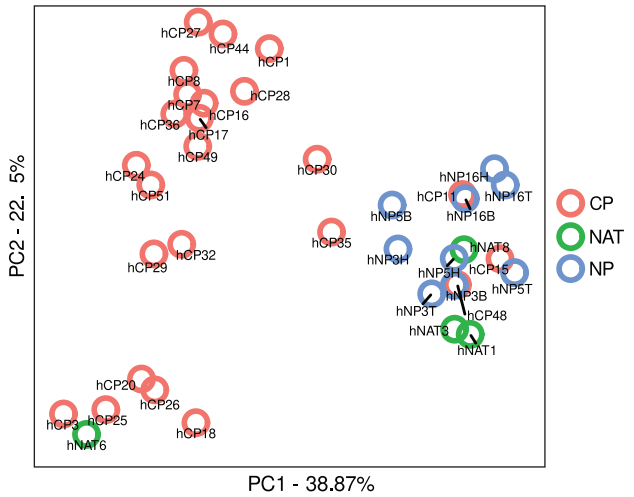


**B.**

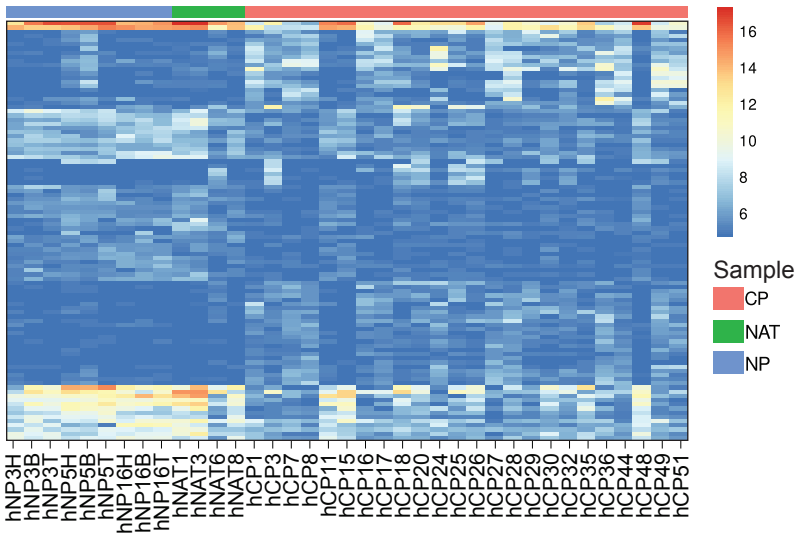


**C.**

**Up**
**CP vs. NP + NAT**

| Gene | log2FC | padj |
|---|---|---|
| FOLH1 | 24.48 | 1.25E-36 |
| GCG | 13.51 | 1.39E-03 |
| PSG4 | 12.30 | 3.27E-20 |
| TMEM132C | 12.01 | 1.14E-06 |
| ENSG00000226278 | 11.79 | 3.88E-05 |
| PEG3 | 11.41 | 1.94E-08 |
| PAH | 10.39 | 7.66E-04 |
| FAM107A | 10.24 | 3.49E-06 |
| NOS2 | 8.10 | 5.86E-05 |
| SLC10A2 | 6.92 | 7.16E-08 |

**Down**
**CP vs. NP + NAT**

| Gene | log2FC | padj |
|---|---|---|
| OSR2 | -4.56 | 3.11E-05 |
| MAP3K20-AS1 | -4.56 | 7.53E-03 |
| LMO3 | -3.77 | 3.36E-02 |
| SOX5 | -3.73 | 1.02E-04 |
| GLP1R | -3.70 | 3.25E-02 |
| CELA3A | -3.67 | 2.02E-03 |
| PIK3CG | -3.67 | 7.64E-03 |
| FUT9 | -3.50 | 1.46E-02 |
| PGC | -3.45 | 1.38E-02 |
| SIX1 | -3.37 | 2.16E-03 |

**D.**

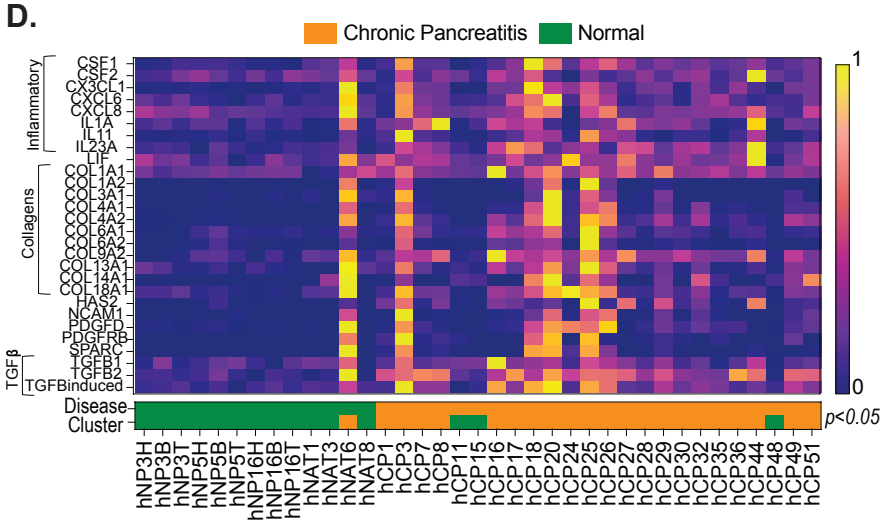


**E.**

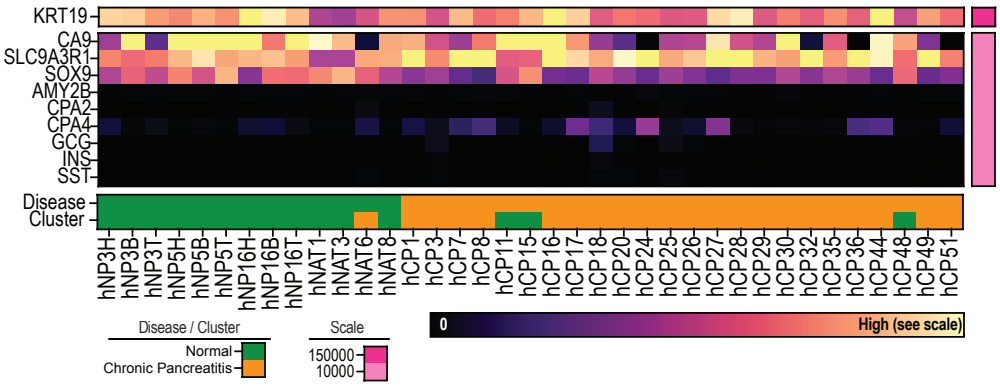


**F.**

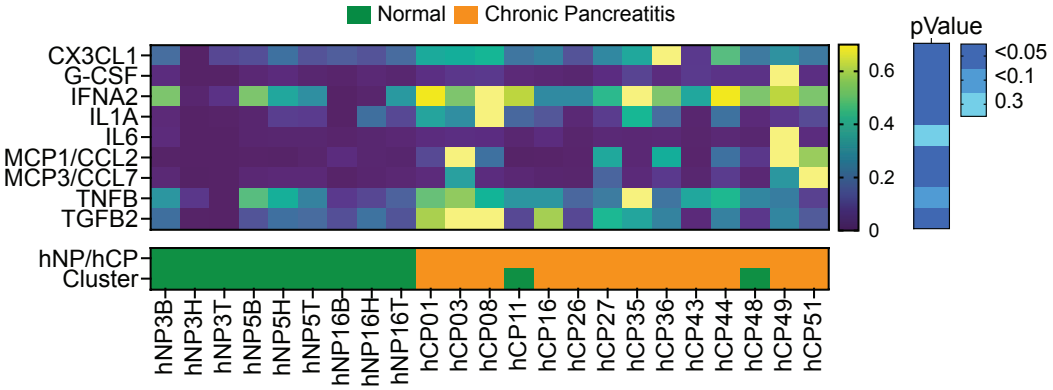

**Figure 4. Transcriptomic analysis reveals subtypes of CP found in patient samples.**

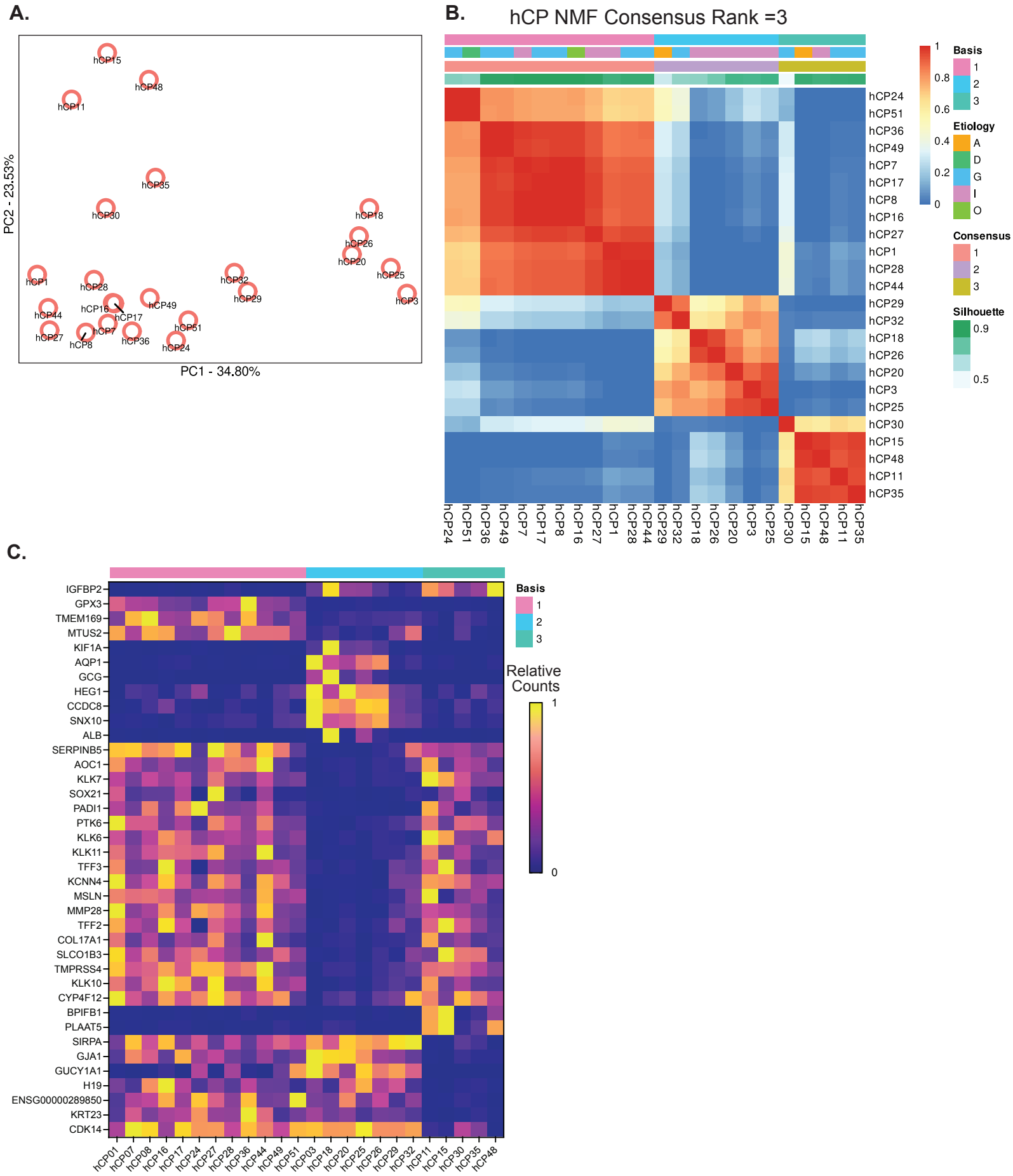
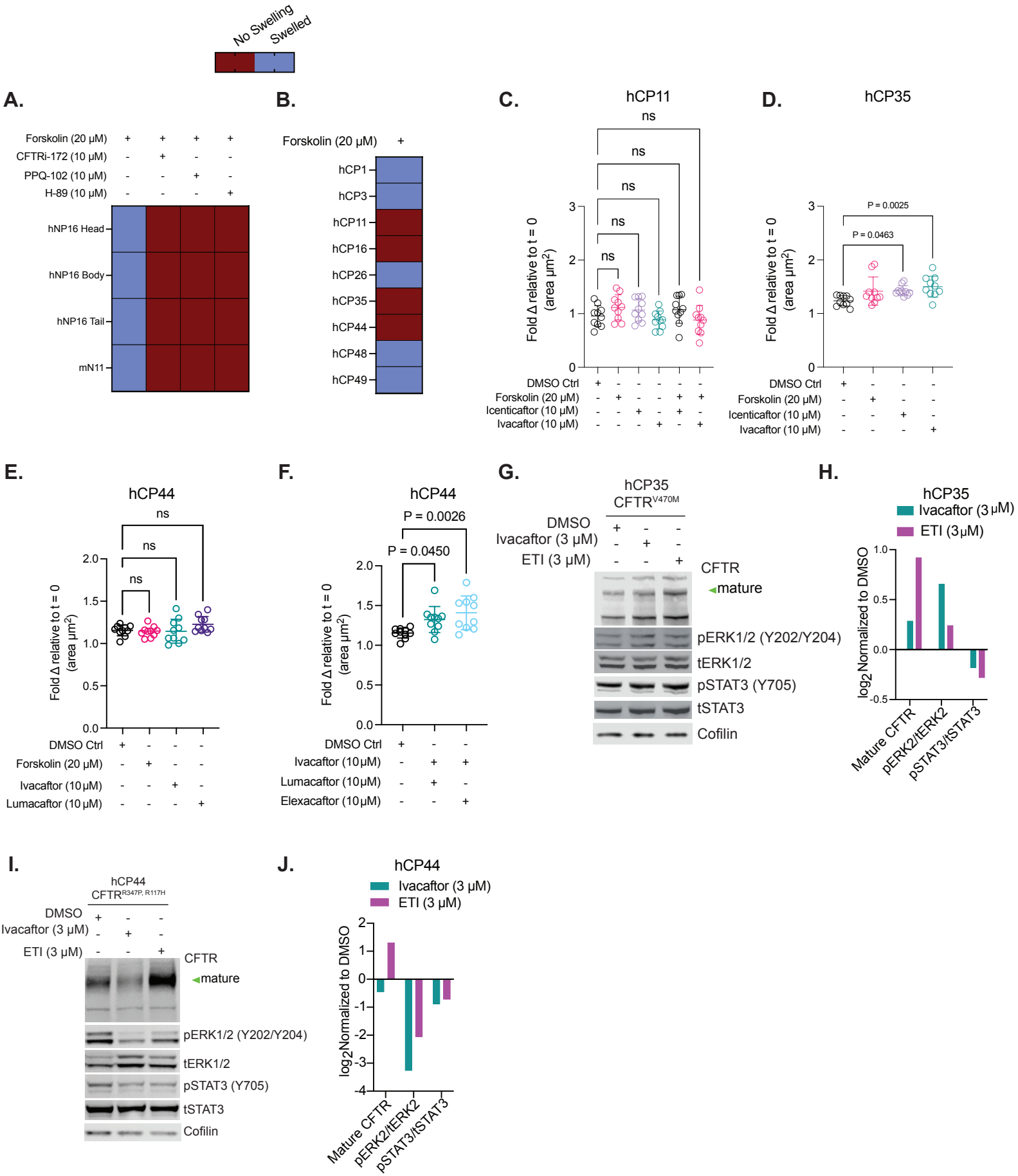
**Figure 5. Cystic fibrosis transductance regulator (CFTR) expression or dependent swelling of CP organoids is resolved upon addition of CFTR modulators, potentiators, or correctors.**